
Bayesian Conformal Prediction as a Decision Risk Problem

Fanyi Wu^{1,2}, Veronika Lohmanova¹, Samuel Kaski^{1,3,4}, Michele Caprio¹

¹Department of Computer Science, University of Manchester, Manchester, UK

²UKRI AI Centre for Doctoral Training in Decision Making for Complex Systems

³Department of Computer Science, Aalto University, Espoo, Finland

⁴ELLIS Institute, Finland

Abstract

We propose an optimised Bayesian Conformal Prediction (BCP) framework that selects the conformal threshold via a decision-theoretic risk minimisation criterion. BCP uses Bayesian posterior predictive densities as non-conformity scores and Bayesian quadrature to estimate and minimise the expected prediction set size. Operating within a split conformal framework, BCP provides valid coverage guarantees and demonstrates reliable empirical coverage under model misspecification. Across regression and classification tasks, including distribution-shifted settings such as ImageNet-A, BCP yields prediction sets of comparable size to split conformal prediction, while exhibiting substantially lower run-to-run variability in set size. In sparse regression with nominal coverage of 80%, BCP achieves 81% empirical coverage under a misspecified prior, whereas Bayesian credible intervals under-cover at 49%.

1 Introduction

Uncertainty quantification is essential for building reliable machine learning systems. While advances like Bayesian inference, deep ensembles, and model calibration have improved uncertainty estimation [Angelopoulos and Bates, 2021, Gal and Ghahramani, 2016, Tyralis and Papacharalampous, 2024, Caprio et al., 2024], these methods often rely on the correctness of the underlying probabilistic model and may fail under misspecification.

In contrast, *Conformal Prediction* (CP) provides finite-sample, distribution-free coverage guarantees under the exchangeability assumption. For any significance level $\alpha \in (0, 1)$, CP aims to construct prediction sets C_{cp} that contain the true outcome with probability at least $1 - \alpha$ [Shafer and Vovk, 2008, Barber et al., 2023, Caprio et al., 2025]. Let $(X_1, Y_1), \dots, (X_{n+1}, Y_{n+1})$ be exchangeable observations. A non-conformity score $s(x, y)$ is a real-valued function that quantifies how atypical a candidate output y is for an input x relative to the observed data, with larger values indicating lower conformity. Given such a score, the prediction set C_{cp} for a new input X_{n+1} is defined as

$$C_{\text{cp}}(x_{n+1}) = \{y \in \mathcal{Y} : s(x_{n+1}, y) \leq \lambda_{\text{cp}}\}, \quad (1)$$

where the threshold λ_{cp} is calibrated from data. Appropriate calibration of λ_{cp} yields valid coverage guarantees; The precise form of the guarantee depends on whether full or split CP is used [Barber et al., 2023].

Beyond validity, a central objective in the CP literature is *efficiency*: constructing prediction regions that are as small as possible while satisfying coverage guarantees [Vovk et al., 2005, Lei et al., 2018, Barber et al., 2023]. Theorem 2.10 in Vovk et al. [2005] shows that, among all valid predictors, there always exists a conformal predictor achieving the same coverage with no larger prediction regions, implying that prediction regions can be improved through the choice of non-conformity score. In

practice, however, most conformal methods rely on fixed quantile calibration of pre-specified scores, rather than explicitly optimising prediction set size under a coverage constraint [Lei et al., 2018, Barber et al., 2023]. Recent studies, summarised in Section 2, have explored connections between CP and Bayesian inference. This raises a natural question: *Can CP be operationalised as a decision-theoretic optimisation problem, in which the conformal threshold λ is treated as a decision variable (of which the classical choice λ_{cp} is a special case) and selected to minimise the expected prediction set size while preserving valid coverage guarantees?*

Contributions

We propose **optimised Bayesian Conformal Prediction (BCP)**. It is, to the best of our knowledge, the first method that explicitly solves an efficiency-coverage optimisation problem for split CP (see Figure 1). Our contributions include:

- **Efficiency-coverage optimisation for split CP.** We present an implementable optimisation procedure in which the conformal threshold λ_{cp} is chosen to minimise the expected prediction set size $\mathbb{E}[|C(X; \lambda)|]$ subject to coverage constraint enforced via conformal risk control (CRC), inspired by the decision-risk perspective of Snell and Griffiths [2025].
- **Bayesian non-conformity scores within split CP.** We use Bayesian posterior predictive densities as non-conformity scores and employ add-one-in (AOI) sampling as a Bayesian score construction and variance-reduction technique (see Appendix C.2).
- **Bayesian quadrature for efficiency optimisation.** We adopt Bayesian quadrature (BQ) to stably estimate the expected prediction set size under input variability, and combine it with the L^+ risk bound to enforce the coverage guarantees that we formalize in (5).

Together, BCP produces prediction sets that minimise the expected prediction-set size over the input distribution, while satisfying coverage guarantees enforced via CRC.

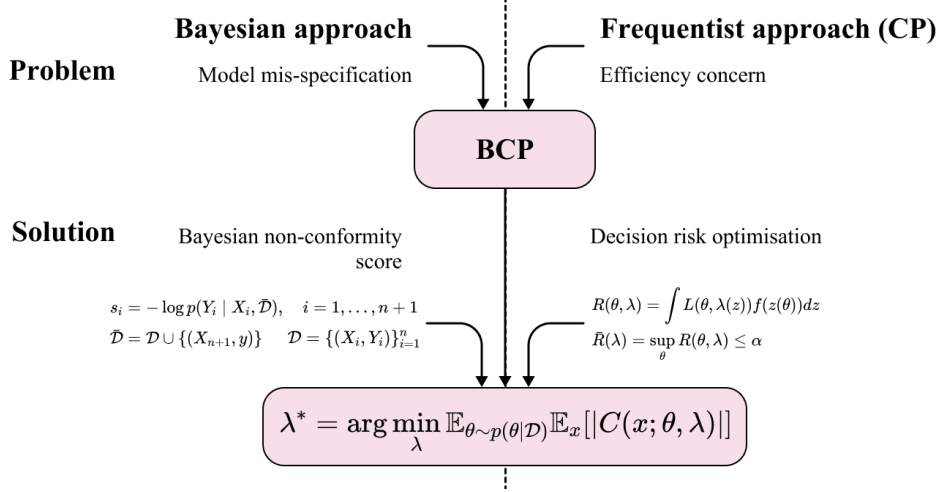


Figure 1: Conceptual overview of BCP. It combines a Bayesian approach with CP through (i) *Bayesian non-conformity scores* constructed via AOI sampling, and (ii) *decision-risk optimisation* based on BQ under CRC.

We evaluate BCP on both regression and classification tasks (Section 5), showing that it empirically achieves the target Probably Approximately Correct (PAC)-style coverage in (5) even under model misspecification, and yields prediction-set size distributions with lower run-to-run variance compared to Bayesian credible intervals and classical split CP.

2 Related Work

CP constructs prediction regions with guaranteed coverage under exchangeability [Vovk et al., 2005, Shafer and Vovk, 2008]. In contrast, Bayesian inference provides calibrated uncertainty when the

model is correct, but can lose coverage under misspecification [Bernardo and Smith, 2009, Jansen, 2013]. Thus, CP and Bayesian inference offer complementary strengths: formal coverage guarantees versus model-based interpretability.

Recent work has attempted to bridge these paradigms. Fong and Holmes [2021] proposed Conformal Bayesian Computation (CB), which uses Bayesian posterior predictive densities as non-conformity scores for full CP, thereby incorporating model uncertainty. Snell and Griffiths [2025] framed split CP as BQ, providing high-probability (PAC-style) coverage guarantees. Conformalized Bayesian Inference (CBI) [Barilett et al., 2025] takes a different approach by applying CP directly to Bayesian posterior distributions in parameter space, yielding valid uncertainty regions for model parameters and derived quantities. Caprio [2025, Section 4] studies under which hypotheses Bayesian reasoning and conformal prediction are equivalent prediction methods.

Theorem 2.10 in Vovk et al. [2005] shows that, for any valid confidence predictor $\mathcal{C}(x)$, there exists a conformal predictor achieving the same coverage with no larger prediction regions (reviewed in Appendix A). This result suggests that, among all valid predictors, one can in principle seek the smallest prediction regions while preserving coverage guarantees.

Building on this perspective, BCP explicitly formulates and solves an optimisation problem within split CP, selecting the threshold λ to minimise the expected prediction-set size $|\mathcal{C}(X; \lambda)|$ while enforcing PAC-style coverage guarantees in (5) via CRC.

3 CP as a Decision Risk Problem

From a decision-theoretic perspective, constructing a CP set corresponds to choosing a threshold λ that balances the risk of miscoverage against the cost of producing larger prediction sets. The miscoverage loss is defined as

$$L(y, \mathcal{C}(x; \lambda)) = \mathbb{I}\{y \notin \mathcal{C}(x; \lambda)\}, \quad (2)$$

where $\mathbb{I}\{\cdot\}$ denotes the indicator function. Formally, we parametrise CP sets by a real-valued threshold $\lambda \in \mathbb{R}$. For a given input x , the resulting prediction set is denoted by $\mathcal{C}(x; \lambda)$.

In classical CP, the threshold λ_{cp} is obtained via empirical quantile calibration and represents a particular feasible choice of λ . In particular, classical CP constructs prediction sets by thresholding a fixed non-conformity score $s(x, y)$, which is independent of model parameters θ and does not involve optimisation over λ beyond the quantile-based choice λ_{cp} . In split CP, the threshold λ_{cp} is given by

$$\lambda_{cp} = s_{(\lceil (n+1)(1-\alpha) \rceil)}, \quad (3)$$

where $s_{(1)} \leq \dots \leq s_{(n)}$ denote the ordered non-conformity scores $s_i = s(X_i, Y_i)$ computed on the calibration data.

In contrast, BCP treats λ as a decision variable and seeks values of λ for which the miscoverage risk

$$R(\lambda) = \mathbb{E}[L(Y, \mathcal{C}(X; \lambda))] \quad (4)$$

is controlled at level α via CRC, rather than enforced through exact marginal coverage as in classical CP. This leads to the PAC-style constrained optimisation problem [Valiant, 1984]:

$$\begin{aligned} \min_{\lambda} \quad & \mathbb{E}_X[|\mathcal{C}(X; \lambda)|] \\ \text{s.t.} \quad & \mathbb{P}_{\mathcal{D}}(\mathbb{P}_{(X, Y)}(Y \notin \mathcal{C}(X; \lambda)) \leq \alpha) \geq 1 - \beta. \end{aligned} \quad (5)$$

Here, $\lambda = \hat{\lambda}(\mathcal{D})$ is calibrated from data $\mathcal{D} = (X_i, Y_i)_{i=1}^n$, $\mathcal{C}(X; \lambda)$ is the prediction set for test input X , and $|\mathcal{C}(X; \lambda)|$ denotes its size. The constraint ensures that with probability at least $1 - \beta$ over random data \mathcal{D} , the test miscoverage $\mathbb{P}_{(X, Y)}\{Y \notin \mathcal{C}(X; \lambda)\}$ does not exceed α .

This decision-risk perspective naturally connects to Bayesian inference. Instead of relying on fixed empirical scores, BCP uses the Bayesian posterior predictive density in (6) as its non-conformity score, thereby incorporating both parameter and predictive uncertainty. Coverage is guaranteed under split CP with CRC, which requires: (i) exchangeability between calibration and test samples, and (ii) the Bayesian model trained on a training set without access to calibration data. The resulting BCP framework combines PAC-style coverage guarantees with Bayesian modelling and optimisation. Formal guarantees are provided in Appendix B.

4 Method

We now implement the decision risk optimisation of CP in (5). We use a Bayesian posterior predictive density as the non-conformity score. Importantly, all non-conformity scores are computed using a scoring rule that is fixed with respect to the calibration labels, ensuring the validity of split CP with CRC. Our method combines three components: (i) AOI sampling for efficient Bayesian non-conformity score computation, (ii) BQ for expectation estimation, and (iii) Dirichlet-based risk control L^+ for valid finite-sample guarantees.

4.1 AOI posterior sampling

Let $D_{\text{tr}} = \{(X_i, Y_i)\}_{i=1}^n$ denote the training dataset. We denote by $p(\theta | D_{\text{tr}})$ the posterior over model parameters θ and by $f_\theta(y | x)$ the conditional data-generating model. Given posterior samples $\{\theta^{(t)}\}_{t=1}^T \sim p(\theta | D_{\text{tr}})$ obtained via MCMC, we use add-one-in (AOI) importance sampling [Fong and Holmes, 2021] to approximate posterior predictive densities without recomputing the posterior for each candidate label.

AOI is used as a numerical approximation to define a posterior predictive scoring rule based on the training data. The posterior is never updated using calibration labels, so the resulting score function is fixed with respect to the calibration set and can be evaluated uniformly on both calibration and test examples, as required by split CP.

For a candidate label y at input x_{n+1} , AOI assigns importance weights

$$\tilde{w}^{(t)} = \frac{f_{\theta^{(t)}}(y | x_{n+1})}{\sum_{t'=1}^T f_{\theta^{(t')}}(y | x_{n+1})}, \quad t = 1, \dots, T, \quad (6)$$

and estimates the posterior predictive density as

$$\hat{p}(y | x, D_{\text{tr}}) = \sum_{t=1}^T \tilde{w}^{(t)} f_{\theta^{(t)}}(y | x). \quad (7)$$

We then define the non-conformity score as

$$s(x, y) = -\log \hat{p}(y | x, D_{\text{tr}}). \quad (8)$$

Because the same scoring rule is applied to calibration and test points, the resulting non-conformity scores are exchangeable conditional on the training data, preserving the validity of split CP.

4.2 Bayesian risk optimisation

We adopt the decision-theoretic view of CP from Snell and Griffiths [2025], in which a decision rule maps inputs to prediction sets and is parametrised here by the conformal threshold λ . For a fixed input x and candidate output y , the resulting prediction set $\mathcal{C}(x; \lambda)$ incurs a pointwise miscoverage loss as in (2). Conditioned on fixed model parameters θ , this induces the conditional risk

$$R(\theta, \lambda) = \int_{\mathcal{X}} \int_{\mathcal{Y}} L(y, \mathcal{C}(x; \lambda)) p(y | x, \theta) p(x) dy dx, \quad (9)$$

where $p(x)$ denotes the test-time input distribution.

Rather than considering a worst-case risk over θ , we use the Bayesian posterior $p(\theta | D_{\text{tr}})$ to define a posterior-averaged risk, which is employed solely as an optimisation objective for selecting the threshold λ :

$$R(\lambda) = \int_{\mathcal{X}} \int_{\mathcal{Y}} \int_{\mathcal{P}} L(y, \mathcal{C}(x; \lambda)) p(y | x, \theta) p(\theta | D_{\text{tr}}) p(x) dx dy d\theta. \quad (10)$$

This posterior-averaged risk is not used to certify coverage guarantees. In our method, formal coverage is enforced separately via the PAC-style CRC constraint in (5). In practice, expectations with respect to the posterior distribution over θ that appear in the optimisation objective are approximated via Monte Carlo integration using posterior samples $\{\theta^{(t)}\}_{t=1}^T$, with AOI reweighting employed to evaluate the corresponding posterior predictive quantities as in (6).

Minimising the miscoverage risk $R(\lambda)$ corresponds to reducing the probability of miscoverage averaged over test-time inputs and posterior uncertainty in the model parameters, which provides a principled rationale for treating the conformal threshold λ as a decision variable.

For our PAC-style constrained optimisation problem in (5), coverage is enforced separately via CRC, and optimisation focuses on efficiency, measured by the expected prediction-set size $\mathbb{E}_X[|\mathcal{C}(X; \lambda)|]$.

4.3 Bayesian Quadrature

The optimisation problem in (5) requires evaluating the input expectation

$$\mathbb{E}_X[|\mathcal{C}(X; \lambda)|] = \int |\mathcal{C}(x; \lambda)| p(x) dx, \quad (11)$$

which is generally intractable due to the unknown input distribution $p(x)$ and the expensive evaluation of the prediction set size $|\mathcal{C}(x; \lambda)|$. While Monte Carlo estimation is in principle sufficient, it can incur high variance when each evaluation of $|\mathcal{C}(x; \lambda)|$ is costly, leading to unstable optimisation of the threshold λ . We therefore employ BQ as a variance reduction tool to estimate stably (11). Following the probabilistic numerics perspective [O'Hagan, 1991], we define the integrand

$$g_\lambda(x) = |\mathcal{C}(x; \lambda)| \quad (12)$$

and, for a fixed value of λ , place a Gaussian process prior over the mapping $x \mapsto g_\lambda(x)$. Given evaluations at selected input locations, BQ yields a posterior distribution over the integral $\mathbb{E}_X[g_\lambda(X)]$, whose mean provides a low-variance estimator and whose uncertainty can be used to guide adaptive evaluation.

The resulting trade-off between coverage and expected prediction set size as a function of λ is illustrated in Figure 2.

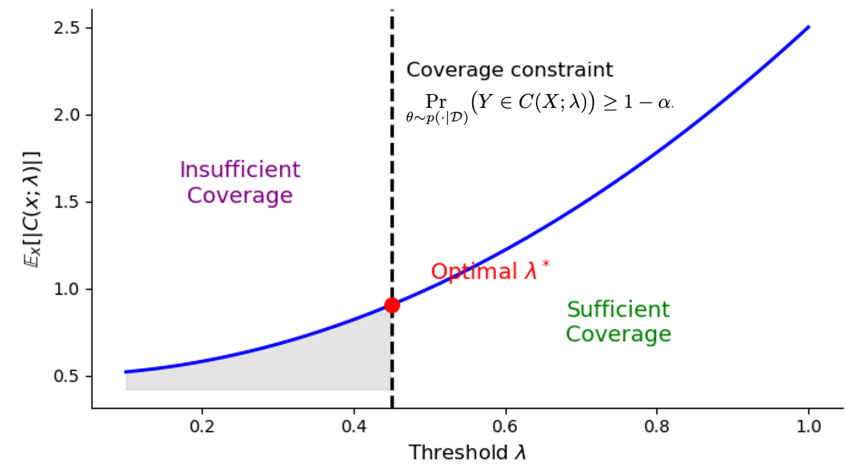


Figure 2: BQ optimisation of the threshold λ under a coverage constraint. The blue curve shows the expected prediction set size $\mathbb{E}_x[|\mathcal{C}(x; \theta, \lambda)|]$ as a function of λ , increasing as more y 's are included. The green dashed line marks the boundary induced by the CRC constraint, beyond which the target coverage level is satisfied with confidence $1 - \beta$. The optimal λ^* is selected as the smallest λ that ensures sufficient coverage while minimising prediction set size.

4.4 Empirical risk control via L^+ .

Direct evaluation of the Bayesian risk in (10) is generally intractable, as it involves expectations over both the data-generating distribution and posterior uncertainty. We therefore adopt the CRC framework [Snell and Griffiths, 2025] and use the L^+ statistic as a computable upper bound on the true miscoverage risk:

$$L^+ = \sum_{i=1}^{n+1} U_i \ell_{(i)}, \quad U \sim \text{Dir}(1, \dots, 1), \quad (13)$$

Algorithm 1 BCP (AOI + BQ + L^+ risk control)

Require: Training data \mathcal{D}_{tr} , calibration data \mathcal{D}_{cal} , test input x_{n+1} , miscoverage level α , confidence level β

Ensure: Prediction set $\mathcal{C}(x_{n+1}; \lambda^*)$

- 1: Draw posterior samples $\{\theta^{(t)}\}_{t=1}^T \sim p(\theta \mid \mathcal{D}_{\text{tr}})$ ▷ fit once on training only
- 2: Using AOI re-weighting, define the posterior predictive score $s(x, y)$ and compute calibration scores $\{s(X_i, Y_i)\}$ for $(X_i, Y_i) \in \mathcal{D}_{\text{cal}}$
- 3: For candidate labels y , compute test scores $s(x_{n+1}, y)$ and the corresponding set $\mathcal{C}(x_{n+1}; \lambda) = \{y : s(x_{n+1}, y) \leq \lambda\}$
- 4: Use BQ to estimate $\mathbb{E}_X[|\mathcal{C}(X; \lambda)|]$ for candidate thresholds λ
- 5: Select λ^* minimising the BQ-estimated set size subject to the CRC L^+ constraint at (α, β)
- 6: **return** $\mathcal{C}(x_{n+1}; \lambda^*)$

where ℓ_i denotes the miscoverage loss on the i -th calibration example $z_i = (X_i, Y_i)$, and $\ell_{(1)} \leq \ell_{(2)} \leq \dots \leq \ell_{(n+1)}$ denote the order statistics of the losses $\{\ell_i\}_{i=1}^{n+1}$. The L^+ statistic stochastically upper-bounds the true miscoverage risk $\mathbb{P}_{(X, Y)}(Y \notin \mathcal{C}(X; \lambda))$ under the exchangeability assumption [Angelopoulos et al., 2025]. We select the smallest λ satisfying

$$\mathbb{P}_{\mathcal{D}}[L^+(\lambda) \leq \alpha] \geq 1 - \beta. \quad (14)$$

which guarantees coverage $1 - \alpha$ with confidence $1 - \beta$ and is typically less conservative than standard CRC.

High-Level View of BCP. BCP draws posterior samples $\{\theta^{(t)}\}_{t=1}^T$ to capture parameter uncertainty and applies AOI reweighting to compute non-conformity scores for calibration and test data. The expected prediction set size $\mathbb{E}_x[|\mathcal{C}(x; \lambda)|]$ is estimated via BQ, integrating over input variability. Coverage is enforced through the Dirichlet-weighted L^+ bound, and the optimal threshold λ^* minimises the BQ-estimated set size under this constraint, yielding the final conformal set $\mathcal{C}(x; \lambda^*)$. Algorithm 1 summarises the procedure, with full details provided in Appendix C.6.

5 Experiments

We evaluate BCP on both regression and classification tasks, comparing it against classical split CP, Conformal Bayesian Computation (CB), and Bayesian Credible Intervals (BCI), and Maximum Softmax Probability (MSP). BCP prioritises valid risk control and stability under model misspecification. It is designed to minimise prediction set size subject to the coverage constraint, and may trade a modest increase in average set size for improved stability in both prediction-set size and empirical coverage across repeated data splits. All experiments are implemented in Python (version 3.14) using libraries such as PyTorch, Pyro, and scikit-learn. Additional implementation details and further experimental results are provided in Appendix D.

5.1 Sparse Regression on the Diabetes Dataset

Following Fong and Holmes [2021], we consider a sparse linear regression model on the diabetes dataset in Efron et al. [2004]. The dataset includes $n=442$ samples with $d=10$ features and a continuous response representing disease progression. The likelihood is Gaussian,

$$f_{\theta}(y \mid x) = \mathcal{N}(y \mid \theta^{\top} x + \theta_0, \tau^2), \quad (15)$$

with hierarchical priors

$$\begin{aligned} \pi(\theta_j) &= \text{Laplace}(0, b), \\ \pi(b) &= \text{Gamma}(1, 1), \\ \pi(\tau) &= \mathcal{N}^+(0, c). \end{aligned} \quad (16)$$

where $c \in \{1.0, 0.02\}$ controls prior concentration. Data are standardised after the train-calibration split to prevent leakage. For both $c = 1.0$ (well-specified) and $c = 0.02$ (misspecified) priors verified by Jansen [2013], posterior samples are obtained via MCMC ($T = 8000$). We compare Split-CP, BCI, CB [Fong and Holmes, 2021], and BCP. In this experiment, AOI reweighting is applied to

Table 1: Regression results on the Diabetes dataset (target coverage: 80%). Comparison across Split CP, Bayesian credible intervals (BCI), Conformal Bayesian Computation (CB), and Bayesian Conformal Prediction (BCP) under two prior scales $c \in \{1.0, 0.02\}$. We highlight serious errors in red, and present BCP results in bold.

Method	c	Cov. (%)	Width	Pred. (s)	Calib. (s)
Split-CP	1.0	78.75	1.80	1.743×10^{-5}	0.002
Split-CP	0.02	78.75	1.81	1.800×10^{-5}	0.001
BCI	1.0	78.47	1.77	5.523×10^{-4}	-
BCI	0.02	49.17	1.00	5.840×10^{-4}	-
CB	1.0	79.26	1.80	1.703×10^{-3}	5.149
CB	0.02	79.20	1.80	1.892×10^{-3}	5.364
BCP	1.0	81.25	1.92	8.595×10^{-4}	39.692
BCP	0.02	80.83	1.90	8.597×10^{-4}	48.316

compute test-time non-conformity scores, while calibration scores are computed using the fixed posterior predictive distribution.

To assess coverage, 50 data splits are performed, with 52.5% for training, 17.5% for calibration, and 30% for testing. For each split, CP intervals are constructed on a grid of 100 values evenly spaced over the interval between the minimum and maximum label values in the training dataset.

BCP refinement. To stably optimise the threshold λ under coverage constraints in (5), we apply the BQ method described in Section 4.3, which yields low-variance estimates of $\mathbb{E}_x[|C(x; \lambda)|]$. We set the miscoverage level $\alpha = 0.2$, and the confidence parameter β is scanned over $[0.6, 0.95]$ for the optimal configuration.

Figure 3 shows that BCP produces prediction regions that satisfy the target coverage constraint while remaining competitive in size compared to CB for both prior scales. While both methods achieve coverage close to the nominal coverage (80%) on average, CB exhibits higher variability across random splits. In contrast, BCP produces a more concentrated coverage distribution, indicating more stable risk control under model misspecification.

Notably, under severe prior misspecification ($c = 0.02$), BCI substantially under-cover (49.2% empirical coverage), despite producing a narrower prediction set. In contrast, BCP restores near-nominal coverage (80.8%) while maintaining prediction set sizes comparable to conformal baselines, highlighting its ability to prioritise validity under model misspecification.

5.2 Breast Cancer Classification

We evaluate sparse binary classification on the Wisconsin breast cancer dataset [Wolberg and Mangasarian, 1990], which contains 569 samples with 30 features and binary labels (benign vs. malignant). We adopt a Bayesian logistic regression model,

$$f_\theta(y=1 \mid x) = (1 + \exp[-(\theta^\top x + \theta_0)])^{-1}, \quad (17)$$

with standard Gaussian priors and target miscoverage level $\alpha = 0.2$.

As discussed in Section 4, we adopt split CP with CRC, which provides PAC-style marginal coverage guarantees. Under this framework, prediction sets are not required to be non-empty for every test input [Lei et al., 2018]. In binary classification, this may result in empty prediction sets for a subset of test points. Accordingly, the reported average set size is the mean cardinality $|C(x)| \in \{0, 1, 2\}$; values below 1 indicate that a fraction of test inputs receive empty prediction sets.

Table 2 reports results averaged over 50 random train/calibration/test splits using a 52.5/17.5/30 partition. Posterior inference is performed via MCMC with $T = 8000$ samples. CB and BCP achieve empirical coverage and prediction set sizes comparable to classical Split-CP, while BCP improves efficiency through posterior-aware threshold selection.

Figure 4 illustrates empirical coverage as a function of the target risk level α and the confidence parameter β . In our formulation, the confidence level is defined as $1 - \beta$ in (14). Consequently,

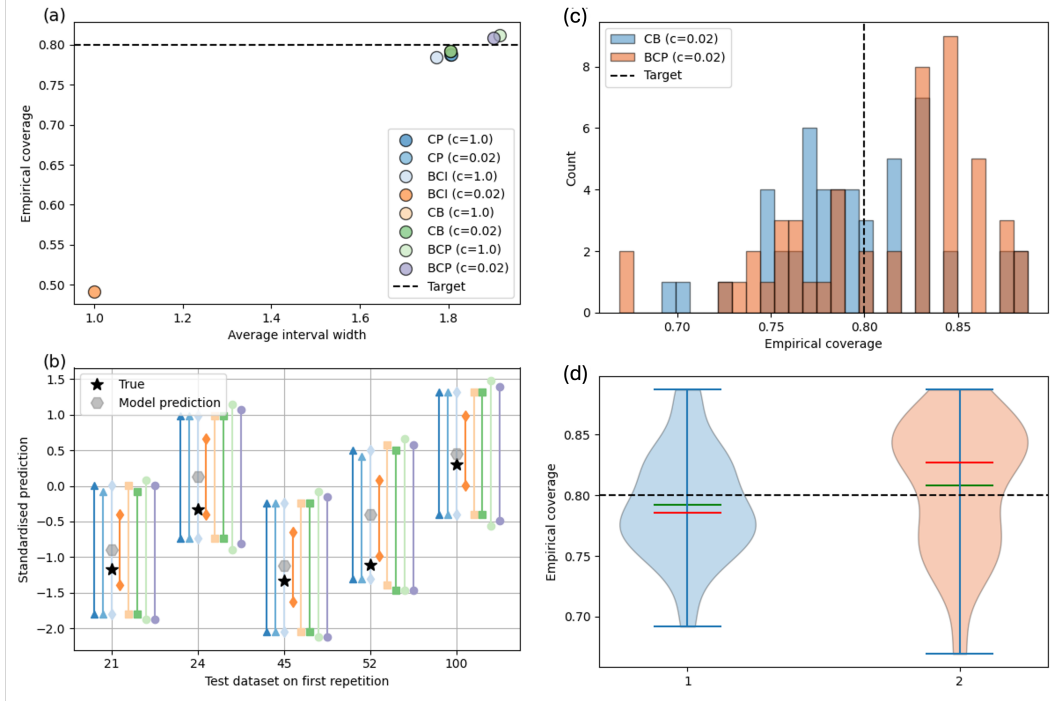


Figure 3: Comparison of prediction regions from CB and BCP methods on a regression task. (a) Empirical coverage versus average interval width for four conformal methods. The dashed line indicates the target coverage level of 80%. (b) Predicted intervals for a random subset of test points from each method, showing interval width and coverage. (c) Histograms of empirical coverage over multiple random splits for CB and BCP, with the dashed line indicating the target coverage level. (d) Violin plots summarising the same distributions, where horizontal red and green markers denote the median and mean, respectively.

Table 2: Classification results (average over 50 random splits, target miscoverage $\alpha = 0.2$). BCI is highlighted in red to indicate substantial overcoverage and overly conservative prediction sets relative to the target risk level. Split CP is in bold for smaller set size while satisfying the target coverage in this experiment.

Method	Cov. (%)	Avg. set size	Pred. (s)	Calib. (s)
Split CP	80.54	0.81	4.849×10^{-5}	0.005
BCI	98.91	1.05	4.916×10^{-5}	-
CB	80.34	0.81	7.197×10^{-4}	6.528
BCP	81.94	0.82	1.385×10^{-4}	11.014

a larger β corresponds to a lower confidence requirement, leading to less conservative thresholds, smaller prediction sets, and potentially lower empirical coverage. In contrast, smaller α enforces stricter risk control and yields more conservative prediction sets.

Overall, both CB and BCP achieve coverage close to the nominal 80% target with prediction set sizes comparable to Split-CP. In contrast, BCI substantially overcovers, reaching nearly 99% coverage with larger average set sizes, highlighting the effect of CP in correcting Bayesian miscalibration. Among the valid methods, BCP attains slightly higher empirical coverage than CB and Split-CP while maintaining similar set sizes. This improvement comes at a moderate additional calibration cost due to posterior sampling.

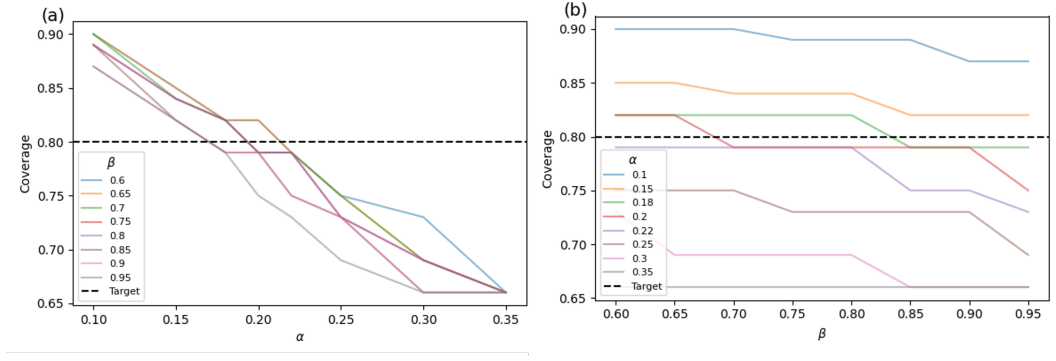


Figure 4: Empirical coverage of Bayesian conformal prediction (BCP) on the breast cancer classification task. (a) Coverage as a function of the target risk level α for different HPD levels β . (b) Coverage as a function of β for different values of α . The dashed horizontal line indicates the target coverage level $1 - \alpha$.

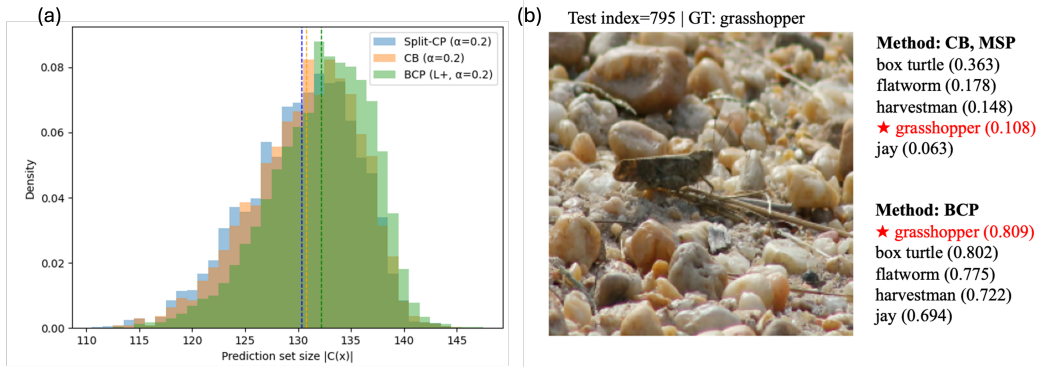


Figure 5: ImageNet-A demo results ($\alpha = 0.2$). (a) Prediction set size distributions on the ImageNet-A test set for Split-CP, CB, and BCP ($\alpha = 0.2$). Dashed lines denote the mean set size of each method. (b) Qualitative comparison on an ImageNet-A test example (index 795, ground truth: *grasshopper*). We show the top-ranked labels and associated scores produced by MSP/CB and BCP. The star indicates the ground-truth class.

5.3 High-dimensional ImageNet-A Classification

To explore the effect of BCP on high-dimensional, more complex datasets, we evaluate the BCP framework on ImageNet-A, a challenging out-of-distribution benchmark designed to test robustness to natural distribution shifts. Our goal on ImageNet-A is to evaluate prediction set quality under epistemic uncertainty and distribution shift, with a fixed backbone representation to isolate effects beyond feature learning.

We use a fixed ImageNet-pretrained ResNet-50 backbone with a Monte Carlo Dropout classification head, and compute AOI-based non-conformity scores from the posterior predictive distribution obtained via multiple stochastic forward passes, following Section 4. We define $s(x, y) = -\log p(y | x, D)$ and set the target miscoverage level to $\alpha = 0.2$.

We partition ImageNet-A into 2,000 training samples, 2,000 calibration samples, and up to 5,000 test samples. The training set is used to fit the dropout head, the calibration set to select the threshold λ , and the test set for evaluation. Due to the high computational cost in this high-dimensional setting, BQ is replaced by empirical risk evaluation over a fixed candidate grid on the calibration set.

We compare CB, split CP, and BCP using empirical coverage and prediction set size on the test set, and analyse the distribution of set sizes across methods. Figure 5 shows the empirical distributions

Table 3: Prediction set statistics on the out-of-distribution ImageNet-A benchmark ($\alpha = 0.2$). BCP results are in bold for improved coverage and stability against random data splits.

Method	Coverage (%)	Cov. std	Mean $ C(x) $	P95 $ C(x) $
Split CP	77.78	0.4158	122.7 ± 5.1	138
CB	79.34	0.4147	123.1 ± 5.0	138
BCP	79.51	0.4108	125.3 ± 4.9	139

of prediction set sizes on ImageNet-A at $\alpha = 0.2$. While all methods achieve comparable coverage by construction, their set size distributions differ markedly. Split-CP and CB exhibit broader distributions, indicating higher variability across test samples. In contrast, BCP produces a more concentrated distribution of set sizes, reflecting reduced variability under posterior-based risk optimisation that explicitly accounts for uncertainty in the predictive distribution, albeit with a slightly larger average set size.

Table 3 reports summary statistics of prediction set sizes on ImageNet-A at $\alpha = 0.2$. All methods achieve comparable empirical coverage close to the target level. Split-CP and CB exhibit nearly identical set size statistics, reflecting their shared quantile-based calibration. BCP attains slightly higher coverage with moderately larger average and upper-quantile set sizes, consistent with its risk-constrained optimisation via the L^+ bound.

Qualitative comparison and scoring methods. For a given ImageNet-A test image, we compute non-conformity scores from the posterior predictive distribution obtained via Monte Carlo Dropout. As a purely Bayesian baseline, Maximum Softmax Probability (MSP) ranks classes according to their posterior predictive probabilities, i.e., $\text{MSP}(x, y) = p(y \mid x, \mathcal{D})$. For visualisation, we list the top-ranked classes and their associated scores under each method, with the ground-truth class highlighted.

We next provide a qualitative comparison under MSP, CB, and BCP on an ImageNet-A test example. All methods rely on the same Bayesian predictive model and posterior samples obtained via Monte Carlo Dropout, but differ in the score functionals used for ranking.

MSP (and CB for visualisation) ranks classes by the posterior predictive mean $p_{\text{mean}}(y \mid x) = \frac{1}{T} \sum_{t=1}^T p_t(y \mid x)$. In contrast, BCP operates on the AOI-based score $p_b(y \mid x) = \frac{\sum_t p_t(y \mid x)^2}{\sum_t p_t(y \mid x)}$, with the conformal threshold calibrated in the p_b score space.

Under MSP/CB, the ground-truth class (*grasshopper*) receives a low posterior-mean score (0.108) and is ranked below several incorrect but visually plausible classes. In contrast, BCP assigns a higher p_b score (0.809) to the ground-truth class and ranks it first, reflecting stronger posterior consistency without modifying the underlying predictive distribution.

Summary and discussion. Across all experiments, BCP consistently enforces the nominal coverage level 80% while exhibiting more stable prediction set behaviour under model misspecification and distribution shift.

In sparse regression, BCP restores near-nominal coverage at the 80% target level under severe prior misspecification, achieving 80.8% empirical coverage where purely Bayesian credible intervals substantially under-cover, and producing prediction sets comparable in size to conformal baselines (split CP and CB). On binary classification tasks, BCP attains empirical coverage close to the 80% target level, with average prediction set sizes comparable to those of Split-CP and CB, and allows for a predictable adjustment of conservativeness through the (α, β) parameters.

On ImageNet-A, Split-CP and CB exhibit nearly identical behaviour, achieving coverage close to the 80% target, but with greater variability in prediction set size across runs. In contrast, BCP produces slightly larger but more stable prediction sets, with reduced variability across runs (Table 3). Figure 5(b) shows that BCP concentrates substantially higher scores on the ground-truth class in challenging cases. This increased stability comes at the cost of additional posterior sampling and calibration overhead, and the choice of (α, β) remains application-dependent.

6 Conclusion

We introduced *optimised Bayesian Conformal Prediction* (BCP), a decision-theoretic framework for conformal prediction that treats the conformal threshold as an explicit decision variable and selects it via posterior-aware risk optimisation, while preserving finite-sample coverage guarantees. By integrating Bayesian posterior predictive scores, BQ for efficient optimisation when computationally feasible, and conformal risk control via the L^+ bound, BCP combines Bayesian structure with frequentist validity in a principled and operational manner.

We compared purely Bayesian methods (BCI, MSP), purely frequentist conformal approaches (Split-CP), and hybrid methods integrating both (CB, BCP), providing insight into how Bayesian structure and frequentist guarantees can be leveraged for reliable uncertainty quantification. Across regression and classification tasks, including settings with model misspecification and distribution shift, BCP achieves reliable coverage together with more stable prediction-set behaviour. In particular, BCP maintains near-nominal coverage under prior misspecification, where Bayesian credible intervals substantially under-cover, while producing prediction sets of comparable size and reduced variability relative to classical conformal baselines.

Conceptually, BCP clarifies a central trade-off in uncertainty quantification: Bayesian assumptions can be exploited to improve efficiency and stability, while conformal calibration retains rigorous, distribution-free validity. In regimes where Bayesian models are informative but imperfect, BCP provides a practical balance between robustness and sharpness, whereas purely distribution-free methods may remain preferable under severe or unstructured misspecification.

Future work includes extensions to high-dimensional and non-parametric Bayesian models, scalable posterior inference and quadrature schemes [Carpenter et al., 2017, Bradbury et al., 2018, Lei, 2019], and applications in safety-critical domains [Wolberg and Mangasarian, 1990, Ovadia et al., 2019, Tyralis and Papacharalampous, 2024].

Impact Statement

This paper presents work whose goal is to advance the field of Machine Learning. There are many potential societal consequences of our work, none which we feel must be specifically highlighted here.

References

Anastasios N. Angelopoulos and Stephen Bates. A gentle introduction to conformal prediction and distribution-free uncertainty quantification, 2021. arXiv preprint.

Anastasios N. Angelopoulos, Stephen Bates, Adam Fisch, Lihua Lei, and Tal Schuster. Conformal risk control, 2025. URL <https://arxiv.org/abs/2208.02814>.

Rina Foygel Barber, Emmanuel J Candes, Aaditya Ramdas, and Ryan J Tibshirani. Conformal prediction beyond exchangeability. *The Annals of Statistics*, 51(2):816–845, 2023.

Nicola Barilett, Nhat Ho, and Alessandro Rinaldo. Conformalized bayesian inference, with applications to random partition models. *arXiv preprint arXiv:2511.05746v1*, 2025. URL <https://arxiv.org/abs/2511.05746v1>.

Jose M Bernardo and Adrian FM Smith. *Bayesian theory*, volume 405. John Wiley & Sons, 2009.

James Bradbury, Roy Frostig, Peter Hawkins, Matthew James Johnson, Chris Leary, Dougal Maclaurin, and Skye Wanderman-Milne. Jax: composable transformations of python+numpy programs. <https://github.com/google/jax>, 2018.

Michele Caprio. The joys of categorical conformal prediction, 2025. URL <https://arxiv.org/abs/2507.04441>.

Michele Caprio, Souradeep Dutta, Kuk Jin Jang, Vivian Lin, Radoslav Ivanov, Oleg Sokolsky, and Insup Lee. Credal bayesian deep learning. *Transactions on Machine Learning Research*, 2024. ISSN 2835-8856. URL <https://openreview.net/forum?id=4NHF9AC5ui>.

Michele Caprio, David Stutz, Shuo Li, and Arnaud Doucet. Conformalized credal regions for classification with ambiguous ground truth. *Transactions on Machine Learning Research*, 2025. ISSN 2835-8856. URL <https://openreview.net/forum?id=L7sQ8CW2FY>.

Bob Carpenter, Andrew Gelman, Matthew D Hoffman, Daniel Lee, Ben Goodrich, Michael Betancourt, Marcus A Brubaker, Jiqiang Guo, Peter Li, and Allen Riddell. Stan: a probabilistic programming language. *Grantee Submission*, 76(1):1–32, 2017.

Bradley Efron, Trevor Hastie, Iain Johnstone, and Robert Tibshirani. Least angle regression. *Annals of Statistics*, 32(2):407–499, 2004.

Edwin Fong and Chris Holmes. Conformal bayesian computation, 2021. URL <https://arxiv.org/abs/2106.06137>.

Yarin Gal and Zoubin Ghahramani. Dropout as a bayesian approximation: Representing model uncertainty in deep learning. In *international conference on machine learning*, pages 1050–1059. PMLR, 2016.

Laurens Jansen. Robust bayesian inference under model misspecification. Master’s thesis, Leiden University, 2013. Chapter 4.5.

Jing Lei. Fast exact conformalization of the lasso using piecewise linear homotopy. *Biometrika*, 106(4):749–764, 2019.

Jing Lei, Max G’Sell, Alessandro Rinaldo, Ryan J. Tibshirani, and Larry Wasserman. Distribution-free predictive inference for regression. *Journal of the American Statistical Association*, 113(523):1094–1111, 2018. doi: 10.1080/01621459.2017.1307116. URL <https://doi.org/10.1080/01621459.2017.1307116>.

Anthony O’Hagan. Bayes–hermite quadrature. *Journal of Statistical Planning and Inference*, 29(3):245–260, 1991.

Yaniv Ovadia, Emily Fertig, Jie Ren, Zachary Nado, David Sculley, Sebastian Nowozin, Joshua Dillon, Balaji Lakshminarayanan, and Jasper Snoek. Can you trust your model’s uncertainty? evaluating predictive uncertainty under dataset shift. *Advances in neural information processing systems*, 32, 2019.

Glenn Shafer and Vladimir Vovk. A tutorial on conformal prediction. *Journal of Machine Learning Research*, 9:371–421, Mar 2008.

Jake C Snell and Thomas L Griffiths. Conformal prediction as bayesian quadrature. *arXiv preprint arXiv:2502.13228*, 2025.

Hristos Tyralis and Georgia Papacharalampous. A review of predictive uncertainty estimation with machine learning. *Artificial Intelligence Review*, 57(4):94, 2024.

L. G. Valiant. A theory of the learnable. *Commun. ACM*, 27(11):1134–1142, November 1984. ISSN 0001-0782. doi: 10.1145/1968.1972. URL <https://doi.org/10.1145/1968.1972>.

Vladimir Vovk, Alex Gammerman, and Glenn Shafer. *Algorithmic Learning in a Random World*. Springer, 2005.

William H. Wolberg and Olvi L. Mangasarian. Multisurface method of pattern separation for medical diagnosis applied to breast cytology. *Proceedings of the National Academy of Sciences*, 87(23):9193–9196, 1990.

A Theoretical Background and Derivations

A.1 Efficiency of Conformal Predictors.

Throughout this appendix, prediction regions are parameterised by a scalar threshold $\lambda \in \mathbb{R}$, and we write $\mathcal{C}(x; \lambda)$ for the induced conformal prediction set. Let $\mathcal{C}(x; \lambda)$ denote a prediction region (or confidence predictor) that maps an input x to a subset of possible outputs.

A classical result by Vovk et al. [2005] states that for any valid predictor $\mathcal{C}(x; \lambda)$ defined on a standard Borel space \mathcal{Z} , there exists a conformal predictor $\mathcal{C}'(x; \lambda)$ such that

$$|\mathcal{C}'(x; \lambda)| \leq |\mathcal{C}(x; \lambda)|, \quad \forall x \in \mathcal{X}, \quad (18)$$

while preserving the same marginal coverage guarantee,

$$\mathbb{P}[Y \in \mathcal{C}'(X; \lambda)] \geq 1 - \alpha, \quad (19)$$

where $|\mathcal{C}(x; \lambda)|$ denotes the size (e.g., interval length or set cardinality) of the prediction region and α is the user-specified miscoverage level. This result implies that, among all predictors achieving a given coverage level, there exists a conformal predictor whose prediction regions are no larger almost surely.

A.2 Expectation-based Formulation.

Both coverage and efficiency can be expressed in expectation form. The marginal coverage can be written as

$$\mathbb{P}[Y \in \mathcal{C}(X; \lambda)] = \mathbb{E}_X[\mathbb{E}_Y[\mathbb{I}\{Y \in \mathcal{C}(X; \lambda)\} \mid X]], \quad (20)$$

while efficiency is measured by the expected prediction set size

$$\text{Eff}(\lambda) := \mathbb{E}[|\mathcal{C}(X; \lambda)|]. \quad (21)$$

This leads to the following constrained optimisation problem:

$$\min_{\lambda} \mathbb{E}[|\mathcal{C}(X; \lambda)|] \quad \text{s.t.} \quad \mathbb{P}[Y \in \mathcal{C}(X; \lambda)] \geq 1 - \alpha. \quad (22)$$

This formulation provides the decision-theoretic foundation for our method. In the main text, this marginal coverage constraint is further strengthened to a PAC-style guarantee via conformal risk control, and the expectation over X is estimated using Bayesian quadrature.

B Theoretical Foundations of the Risk Formulation

B.1 Split Conformal Prediction as Risk Control

Let $z = (x, y)$ denote an input–output pair with $x \in \mathcal{X}$ and $y \in \mathcal{Y}$, and let $\mathcal{D} = \{(X_i, Y_i)\}_{i=1}^n$ denote the observed data. We consider prediction regions parameterised by a scalar threshold λ , denoted by $\mathcal{C}(x; \lambda)$.

We define the miscoverage loss

$$L(y, \mathcal{C}(x; \lambda)) = \mathbb{I}\{y \notin \mathcal{C}(x; \lambda)\}, \quad (23)$$

and the corresponding *data-dependent miscoverage risk*

$$R_{\mathcal{D}}(\lambda) = \mathbb{P}_{(X, Y)}(Y \notin \mathcal{C}(X; \lambda)), \quad (24)$$

where the probability is taken with respect to a fresh test pair (X, Y) drawn exchangeably with the calibration data, conditional on the training data.

In split conformal prediction, the non-conformity score function is fixed with respect to the calibration labels, and the threshold λ is selected using the calibration data only. Rather than enforcing marginal coverage deterministically, we adopt the conformal risk control (CRC) framework [Snell and Griffiths, 2025], which guarantees that

$$\mathbb{P}_{\mathcal{D}}(R_{\mathcal{D}}(\lambda) \leq \alpha) \geq 1 - \beta, \quad (25)$$

for user-specified risk level α and confidence parameter β . This PAC-style guarantee forms the basis of the coverage control used throughout the main text.

B.2 Bayesian Non-conformity Scores under Split Conformal Prediction

Classical non-conformity scores often ignore uncertainty in model parameters. In this work, we define a Bayesian predictive score based on a posterior trained exclusively on the training data:

$$s(x, y) = -\log p(y | x, \mathcal{D}_{\text{tr}}) = -\log \int f_{\theta}(y | x) \pi(\theta | \mathcal{D}_{\text{tr}}) d\theta, \quad (26)$$

where \mathcal{D}_{tr} denotes the training dataset and $\pi(\theta | \mathcal{D}_{\text{tr}})$ is the corresponding posterior. Importantly, this score function is fixed with respect to the calibration and test labels, satisfying the fundamental requirement of split conformal prediction.

Proposition 1 (Validity of Bayesian Scores under Split CP) *Assume that the calibration and test samples are exchangeable conditional on the training data, and that the score function (26) is fixed with respect to the calibration labels. Let λ be selected using conformal risk control applied to the resulting calibration losses. Then the resulting conformal predictor satisfies the PAC-style guarantee (25).*

Proof. Let the training data be \mathcal{D}_{tr} , the calibration data be $\mathcal{D}_{\text{cal}} = \{Z_i\}_{i=1}^n$ with $Z_i = (X_i, Y_i)$, and the test point be $Z_{n+1} = (X_{n+1}, Y_{n+1})$. By assumption, conditional on \mathcal{D}_{tr} , the random variables Z_1, \dots, Z_n, Z_{n+1} are exchangeable.

Define the Bayesian score function $s(x, y) = -\log p(y | x, \mathcal{D}_{\text{tr}})$ as in (26). Since $\pi(\theta | \mathcal{D}_{\text{tr}})$ depends only on \mathcal{D}_{tr} , the score function s is $\sigma(\mathcal{D}_{\text{tr}})$ -measurable and does not depend on any calibration labels $\{Y_i\}_{i=1}^n$. Hence, for any threshold λ , the (miscoverage) loss on an example $z = (x, y)$,

$$\ell(z, \lambda) := \mathbb{I}\{y \notin C(x; \lambda)\}, \quad C(x; \lambda) = \{y' \in \mathcal{Y} : s(x, y') \leq \lambda\},$$

is also $\sigma(\mathcal{D}_{\text{tr}})$ -measurable as a function of z and λ .

Therefore, conditional on \mathcal{D}_{tr} , the random variables $\ell(Z_1, \lambda), \dots, \ell(Z_n, \lambda), \ell(Z_{n+1}, \lambda)$ are exchangeable for each fixed λ . In particular, the calibration losses $\{\ell(Z_i, \lambda)\}_{i=1}^n$ are i.i.d. conditional on \mathcal{D}_{tr} (equivalently, exchangeable with a common conditional law).

Let $\widehat{\lambda} = \widehat{\lambda}(\mathcal{D}_{\text{cal}})$ be the threshold selected by conformal risk control (CRC) applied to the calibration losses induced by s . By the CRC guarantee of Snell and Griffiths [2025] (applied conditional on \mathcal{D}_{tr}), we have

$$\mathbb{P}_{\mathcal{D}_{\text{cal}}} \left(R(\widehat{\lambda}) \leq \alpha \mid \mathcal{D}_{\text{tr}} \right) \geq 1 - \beta,$$

where $R(\lambda) = \mathbb{P}(Y \notin C(X; \lambda) | \mathcal{D}_{\text{tr}})$ denotes the (test-time) miscoverage risk under the exchangeable draw of (X, Y) . Removing the conditioning on \mathcal{D}_{tr} yields the PAC-style statement (25). \square

B.3 Bayesian Risk as an Optimisation Objective

While coverage is enforced via conformal risk control, Bayesian structure is used to guide the selection of the threshold λ through an efficiency-oriented objective. We define the Bayesian decision risk

$$\mathcal{R}(\lambda) = \mathbb{E}_{\theta \sim \pi(\cdot | \mathcal{D}_{\text{tr}})} \mathbb{E}_{X, Y \sim p(\cdot | \theta)} [L(Y, \mathcal{C}(X; \lambda))], \quad (27)$$

which averages miscoverage over posterior uncertainty and the test input distribution.

Minimising the expected prediction set size

$$\mathbb{E}_X [|\mathcal{C}(X; \lambda)|] \quad (28)$$

under the constraint (25) yields the decision-theoretic optimisation problem studied in the main text. In practice, the expectation of X is approximated using Bayesian quadrature, while the Bayesian risk (27) serves solely as an optimisation criterion, and does not provide coverage guarantees.

C Bayesian Risk Estimation and AOI Implementation

C.1 AOI-Based Predictive Scores under Split Conformal Prediction

Let $\mathcal{D}_{\text{tr}} = \{(X_i, Y_i)\}_{i=1}^{n_{\text{tr}}}$ denote the training dataset used to construct a Bayesian posterior $\pi(\theta | \mathcal{D}_{\text{tr}})$. Throughout this appendix, the posterior distribution is fixed with respect to the calibration and test labels.

Given posterior samples $\{\theta^{(t)}\}_{t=1}^T \sim \pi(\theta \mid \mathcal{D}_{\text{tr}})$, we define an AOI-based predictive score for a candidate label y at input x via importance reweighting,

$$\tilde{w}^{(t)}(x, y) = \frac{f_{\theta^{(t)}}(y \mid x)}{\sum_{t'=1}^T f_{\theta^{(t')}}(y \mid x)}, \quad t = 1, \dots, T, \quad (29)$$

and the corresponding predictive density

$$\hat{p}(y \mid x, \mathcal{D}_{\text{tr}}) = \sum_{t=1}^T \tilde{w}^{(t)}(x, y) f_{\theta^{(t)}}(y \mid x). \quad (30)$$

The resulting non-conformity score is

$$s(x, y) = -\log \hat{p}(y \mid x, \mathcal{D}_{\text{tr}}). \quad (31)$$

This construction is motivated by the add-one-in (AOI) sampling [Fong and Holmes, 2021], but crucially does not update the posterior using calibration or test labels. As a result, the score function (31) is fixed with respect to the calibration data, satisfying the requirements of split conformal prediction.

C.2 Exchangeability and Validity

Because the posterior $\pi(\theta \mid \mathcal{D}_{\text{tr}})$ is fixed, the induced score function $s(x, y)$ in (31) is applied identically to all calibration and test points. Assuming exchangeability between the calibration and test samples conditional on the training data, the calibration losses are i.i.d. given \mathcal{D}_{tr} .

Consequently, the conformal risk control guarantees derived in Section B apply directly, and the resulting prediction sets satisfy the PAC-style coverage guarantee

$$\mathbb{P}_{\mathcal{D}}(\mathbb{P}(Y \notin \mathcal{C}(X; \lambda)) \leq \alpha) \geq 1 - \beta. \quad (32)$$

C.3 Importance Sampling Approximation

AOI is approximated via reweighting of posterior draws:

$$\pi(\theta \mid \mathcal{D}_{\text{tr}} \cup \{(x_{n+1}, y)\}) \propto \pi(\theta \mid \mathcal{D}_{\text{tr}}) f_{\theta}(y \mid x_{n+1}), \quad \tilde{w}^{(t)} = \frac{f_{\theta^{(t)}}(y \mid x_{n+1})}{\sum_{t'} f_{\theta^{(t')}}(y \mid x_{n+1})}. \quad (33)$$

The posterior predictive under the augmented dataset becomes

$$\hat{p}(Y_i \mid X_i, \mathcal{D}_{\text{tr}}) = \sum_{t=1}^T \tilde{w}^{(t)} f_{\theta^{(t)}}(Y_i \mid X_i). \quad (34)$$

Each score $s_i = -\log \hat{p}(Y_i \mid X_i, \mathcal{D}_{\text{tr}})$ is thus computed symmetrically for all samples.

C.4 Bayesian Risk as an Optimisation Objective

Bayesian structure is used to guide the selection of the conformal threshold λ through an efficiency-oriented objective. We define the Bayesian decision risk

$$\mathcal{R}(\lambda) = \mathbb{E}_{\theta \sim \pi(\cdot \mid \mathcal{D}_{\text{tr}})} \mathbb{E}_{X, Y \sim p(\cdot \mid \theta)} [L(Y, \mathcal{C}(X; \lambda))], \quad (35)$$

which averages miscoverage over posterior uncertainty and the test input distribution.

Minimising the expected prediction set size $\mathbb{E}_X [\mathcal{C}(X; \lambda)]$ under the PAC-style constraint enforced via conformal risk control yields the optimisation problem studied in the main text. Importantly, the Bayesian risk (35) is used solely as an optimisation criterion and does not provide coverage guarantees.

C.5 Risk Control via L^+

Conformal Risk Control estimates the empirical risk $\hat{R}_n(\lambda) = n^{-1} \sum_i \ell(z_i, \lambda)$, augmented by the stochastic bound

$$L^+ = \sum_{i=1}^{n+1} U_i \ell_{(i)}, \quad U \sim \text{Dir}(1, \dots, 1), \quad (36)$$

which stochastically dominates the posterior risk. The valid threshold satisfies

$$\mathbb{P}_{\mathcal{D}}(\mathbb{P}_{(X,Y)}(Y \notin \mathcal{C}(X; \lambda)) \leq \alpha) \geq 1 - \beta, \quad (37)$$

guaranteeing $(1 - \alpha)$ coverage with confidence $(1 - \beta)$.

C.6 Full BCP–AOI–BQ Algorithm

Algorithm 2 expands all implementation details of the main text procedure.

D Experimental Details and Extended Results

Regression setup. We use the diabetes dataset ($n=442$, $d=10$) with a Gaussian likelihood and a Laplace prior on weights, following Fong and Holmes [2021]. The prior hyperparameter c controls the noise scale’s prior precision: $c=1.0$ (well-specified) and $c=0.02$ (misspecified). Standardisation is applied after splitting to avoid leakage. MCMC is run with 8,000 iterations, discarding the first 2,000 as burn-in. Conformal methods use residual-based scores from Lasso with $\lambda=0.004$. Coverage and width are averaged over 50 splits.

Classification setup. We use the breast cancer dataset ($n=569$, $d=30$), standardised features, and Bayesian logistic regression with Gaussian priors. The training, calibration, and test sets are split in a 52.5/17.5/30 ratio. For each test input, the BCP predictive set is defined as the smallest subset of $\{0, 1\}$ achieving posterior predictive mass $\geq 1 - \alpha$ under the HPD constraint. Empirical coverage and prediction set size are averaged over 50 random seeds. BCP improves efficiency while preserving coverage at $\alpha=0.18$ and $\beta=0.85$.

D.1 Empirical Conservativeness of the L^+ Bound

To investigate the practical conservativeness of the L^+ risk bound, we report in Table 4 the empirical coverage, miscoverage, gap to the nominal target, and the resulting interval width on the Diabetes regression task for fixed $\alpha = 0.20$ and varying β values. These results were computed using the same calibration procedure as in the main text.

Table 4: L^+ conservativeness analysis on the Diabetes dataset ($\alpha = 0.20$). All values are reported with three significant figures. Means are shown with \pm one standard deviation.

β	Coverage	Interval Width	Miscoverage	Gap ($\alpha - \text{mis.}$)
0.60	0.808 ± 0.07	1.82 ± 0.2	0.192	+0.0078
0.65	0.805 ± 0.07	1.80 ± 0.2	0.195	+0.0045
0.70	0.790 ± 0.07	1.75 ± 0.2	0.210	-0.0101
0.80	0.771 ± 0.07	1.67 ± 0.2	0.229	-0.0289
0.90	0.750 ± 0.07	1.61 ± 0.2	0.250	-0.0498

We report the empirical mean and standard deviation across 50 random data splits. Coverage and interval width ($|\mathcal{C}(x)|$) are shown as mean \pm std. Miscoverage is defined as $1 - \text{coverage}$. The last column reports the conservativeness gap $\alpha - \text{miscoverage}$: positive values indicate slight conservativeness (empirical miscoverage below $\alpha = 0.20$), while negative values indicate under-coverage.

Algorithm 2 BCP with AOI-Based Scores and BQ– L^+ Optimisation

Require: Training data $\mathcal{D}_{\text{tr}} = \{(X_i, Y_i)\}_{i=1}^{n_{\text{tr}}}$, calibration data $\mathcal{D}_{\text{cal}} = \{(X_i, Y_i)\}_{i=1}^n$, test input x_{n+1} , miscoverage level α , confidence level β , posterior sample size T , loss bound B , label candidates $\mathcal{Y}_{\text{cand}}$.

1: **Posterior sampling (training only):** Draw $\{\theta^{(t)}\}_{t=1}^T \sim p(\theta \mid \mathcal{D}_{\text{tr}})$.

2: **function** AOI-REWEIGHT($x, y, \{\theta^{(t)}\}$)

3: **for** $t = 1, \dots, T$ **do**

4: $w_t \leftarrow p(y \mid x, \theta^{(t)})$

5: **end for**

6: Normalize weights: $\tilde{w}_t \leftarrow w_t / \sum_{t'=1}^T w_{t'}$

7: **return** $\{\tilde{w}_t\}_{t=1}^T$

8: **end function**

9: **function** COMPUTESCORE(x, y)

10: $\{\tilde{w}_t\} \leftarrow \text{AOI-REWEIGHT}(x, y, \{\theta^{(t)}\})$

11: **return** $-\log \sum_{t=1}^T \tilde{w}_t p(y \mid x, \theta^{(t)})$

12: **end function**

13: **Calibration scores:**

14: **for** $(X_i, Y_i) \in \mathcal{D}_{\text{cal}}$ **do**

15: $s_i \leftarrow \text{COMPUTESCORE}(X_i, Y_i)$

16: **end for**

17: **Test scores:**

18: **for all** $y \in \mathcal{Y}_{\text{cand}}$ **do**

19: $s_{n+1}(y) \leftarrow \text{COMPUTESCORE}(x_{n+1}, y)$

20: **end for**

21: **function** BUILDCONFORMALSET(x, λ)

22: **return** $\{y \in \mathcal{Y}_{\text{cand}} : s(x, y) \leq \lambda\}$

23: **end function**

24: **function** BQ-ESTIMATOR(λ)

25: **return** GP–BQ estimate of $\mathbb{E}_x[|\mathcal{C}(x; \lambda)|]$

26: **end function**

27: **function** COMPUTE- L^+ ($\{\ell_i\}, B$)

28: Sort losses: $\ell_{(1)} \leq \dots \leq \ell_{(n+1)}$

29: Sample $(U_1, \dots, U_{n+1}) \sim \text{Dir}(1, \dots, 1)$

30: **return** $\sum_{i=1}^n U_i \ell_{(i)} + U_{n+1} B$

31: **end function**

32: **BQ-guided candidate search:** Generate a candidate set Λ_{cand} using Bayesian quadrature.

33: **Risk-constrained selection of λ^* :**

34: **for all** $\lambda \in \Lambda_{\text{cand}}$ **do**

35: $\hat{R}_{\text{BQ}}(\lambda) \leftarrow \text{BQ-ESTIMATOR}(\lambda)$

36: **for** $(X_i, Y_i) \in \mathcal{D}_{\text{cal}}$ **do**

37: $\mathcal{C}_i(\lambda) \leftarrow \text{BUILDCONFORMALSET}(X_i, \lambda)$

38: $\ell_i(\lambda) \leftarrow \mathbb{I}\{Y_i \notin \mathcal{C}_i(\lambda)\}$

39: **end for**

40: Generate samples $\{L_m^+(\lambda)\}$ via COMPUTE- L^+ ($\{\ell_i(\lambda)\}, B$)

41: Check feasibility: $\mathbb{P}[L^+(\lambda) \leq \alpha] \geq 1 - \beta$

42: **end for**

$\lambda^* \leftarrow \arg \min_{\lambda \in \Lambda_{\text{cand}}} \hat{R}_{\text{BQ}}(\lambda)$ s.t. validity holds

return $\mathcal{C}(x_{n+1}; \lambda^*) \leftarrow \text{BUILDCONFORMALSET}(x_{n+1}, \lambda^*)$
